

## Isoelectronic impurity states in direct-gap III-V compounds: The case of InP:Bi

W. Rühle, W. Schmid, R. Meck,\* N. Stath,<sup>†</sup> J. U. Fischbach,<sup>‡</sup> I. Strottner, K. W. Benz, and M. Pilkuhn

*Physikalisches Institut, Teil 4, Universität Stuttgart, Pfaffenwaldring 57, D 7000 Stuttgart 80, Germany*

(Received 15 March 1977)

The isoelectronic impurity Bi in the direct-gap III-V compound InP is studied by emission and absorption spectroscopy including magnetic-field, time-resolved, temperature- and excitation-dependent measurements. Doping with Bi gives rise to two emission lines, a sharp Bi "bound exciton"  $(\text{Bi}, X)$  and a broader  $(\text{Bi}, X)$ - $(\text{Bi}, X)$  bound-excitonic molecule. The hole of the bound Bi-exciton is extremely localized while the electron has a typical donorlike Bohr radius. Therefore the  $\text{Bi}^+$  behaves like a pseudodonor, in particular, in magnetoluminescence experiments. The  $(\text{Bi}, X)$ - $(\text{Bi}, X)$  bound-excitonic molecules resemble an  $\text{H}_2$ -like "pseudodonor molecule." This new type of isoelectronic complex is investigated and discussed in detail.

### I. INTRODUCTION

If the anion in compound semiconductors is replaced by another atom of the same group of the Periodic Table, the resulting isoelectronic impurity may have profound influence on the recombination processes. In some cases, these isoelectronic impurities are able to bind electrons or holes due to differences in the atomic pseudopotentials.<sup>1</sup> However, large discrepancies between experimental binding energies and those calculated from the differences of the atomic pseudopotentials are observed. Obviously, deformation of the host lattice has a strong influence on the localization energy of the electron or hole, respectively.

In GaP two types of isoelectronic traps have been carefully investigated: GaP:N, a donorlike isoelectronic trap,<sup>2</sup> and GaP:Bi, an acceptorlike isoelectronic trap.<sup>3</sup> Their significant features are short-range potentials by which the electron or hole are bound. This strongly localized state significantly increases quantum efficiency of recombination in indirect-gap materials like GaP.<sup>4</sup>

In the direct-gap III-V compounds very few investigations of isoelectronic impurities have been reported, and InP:Bi is the only example.<sup>5</sup> The experimental results so far indicate that Bi is a point defect giving rise to a pronounced phonon participation in the direct-recombination process.<sup>5</sup> The main experimental feature of InP doped with Bi is a sharp emission line at 1.3962 eV previously interpreted as a bound-exciton decay<sup>5</sup>  $(\text{Bi}, X)$ . This line has been investigated in Zeeman spectroscopy.<sup>6</sup>

In addition, in this paper we report a second emission band called  $(\text{Bi}, X)_2$  which is always associated with Bi and observed at the low-energy side of the Bi-exciton  $(\text{Bi}, X)$ . A careful experimental investigation of the  $(\text{Bi}, X)$  as well as the  $(\text{Bi}, X)_2$  emission leads to a detailed physical de-

scription of the isoelectronic trap Bi in InP. In particular, we show that the usually adopted picture of a Bi-bound "exciton" describes the physical situation unsatisfactorily. Instead we suggest a localized excitation described by a "pseudodonor model." In this model the hole is extremely localized at the Bi atom and the electron is bound in the Coulomb field of this pointlike positive charge. The wave function of the bound electron is equal to that of a shallow donor.

The following new experimental results support this model. (a) The diamagnetic shift of the Bi-bound "exciton" up to 10 T is exactly that of a donor in InP. (b) The decay times of the Bi emission are much larger (some hundred nanoseconds!) than those of acceptor- or donor-bound excitons ( $A^0, X$  and  $D^0, X$ ) in direct-gap materials (a few nsec in InP).<sup>7</sup> (c) In contrast to the  $(A^0, X)$ - and  $(D^0, X)$ -bound excitons, in InP the Bi "exciton" exhibits a very small oscillator strength in absorption. The last two results are expected for a strongly localized hole state because in this case the overlap with the very wide spread electron wave function is very small. (d) The temperature behavior of the line intensity exhibits an activation energy equal to the donor-binding energy.

In an elegant way the emission  $(\text{Bi}, X)_2$  at the low-energy side of the  $(\text{Bi}, X)$  line can easily be interpreted as the decay of "pseudodonor molecules." These "molecules" are pairs of pseudodonors, the electron energy of which is reduced by the binding energy of the molecule—in direct analogy to the  $\text{H}_2$  molecule.

### II. EXPERIMENTAL

#### A. Growth of InP:Bi epitaxial layers

Epitaxial layers of InP:Bi were grown on (111) and (100) oriented InP substrates by vapor-phase epitaxy (VPE) and by liquid-phase epitaxy (LPE). For the VPE process, a  $\text{PCl}_3$  phosphorous and a

metallic indium source were used.<sup>8</sup> The In-source temperature was 750 °C, whereas the temperature of the substrate was kept at 650 °C. In order to dope the layers, controlled quantities of Bi vapor were added to the main gas stream by evaporating solid Bi contained in a quartz boat at 750 °C. The growth rates of the layers were reduced drastically with increasing amount of Bi vapor in the gas flow.<sup>6</sup>

The LPE layers of InP:Bi were grown by using a horizontal tipping system.<sup>9</sup> Before carrying out the doping experiments with Bi, high-purity InP layers were grown in order to test the purity of the whole epitaxial system.

Bi has a good solubility in In.<sup>10</sup> Bi concentrations ranging from 0.07% to 7% by weight in the solution were used. From the integrated absorption and from the saturation of the Bi luminescence with increasing excitation, the Bi concentration in the samples can be roughly estimated to be  $N_{\text{Bi}} \approx 5 \times 10^{15} - 5 \times 10^{17} \text{ cm}^{-3}$ . The growth temperatures varied between 600 and 700 °C. There is no significant difference between undoped InP LPE layers<sup>9</sup> and InP:Bi LPE layers comparing the growth behavior and the structure of the surface.

#### B. Measurement techniques

The following optical experiments were used to characterize the Bi-related excitation states.

(i) The photoluminescence was measured at low temperatures, with the samples immersed in liquid helium, usually pumped below the  $\lambda$  point. The luminescence light was dispersed by a 1- or 1.5-m grating monochromator and detected by a cooled photomultiplier with S1 cathode. The temperature dependence of the spectra were taken using a temperature-controlled helium-gas-flow cryostat.

(ii) Zeeman spectroscopy was carried out with a superconductive split-coil magnet with a maximum field of 10 T. Both Faraday and Voigt configurations were possible. The linear polarizers were HN7 Kodak polarization sheets, the circular analyzers were constructed by combining two plastic retardation sheets.

(iii) For the time-resolved measurements, a cavity-dumped Ar<sup>+</sup> laser with a pulse duration of 10 nsec and a repetition rate of 50 kHz was used for excitation. Two kinds of measurements have been performed: (a) spectra were taken at different times after the excitation pulse using conventional boxcar technique (gate width 25 nsec); and (b) the time dependence of the luminescence at several fixed wavelengths was recorded by means of a statistical single-photon counting system.

(iv) In addition, absorption experiments at low

temperatures (1.6 K) were performed. In this case the sample used was an epitaxial layer of about 80- $\mu\text{m}$  thickness. By a special etching technique<sup>11</sup> an optical window was etched into the sample by completely removing the substrate.

### III. RESULTS AND DISCUSSION

Figure 1 shows the low-temperature luminescence of three InP samples containing different amounts of Bi (highest Bi concentration for the top spectrum). The intensity of the  $(\text{Bi}, X)$  emission as well as that of the newly reported  $(\text{Bi}, X)_2$  emission increases strongly with Bi concentration. The simultaneously observed  $(D^0, X)$ - and  $(A^0, X)$ -bound exciton and the free-exciton (FE) emission decrease with increasing Bi concentration. Section III A deals with the experimental results and discussion of the Bi exciton  $(\text{Bi}, X)$  at 1.3962 eV; Sec. III B with the  $(\text{Bi}, X)_2$  emission.

#### A. $(\text{Bi}, X)$ emission

##### 1. Magnetic-field experiments

Figure 2 shows the Zeeman splitting of the  $(\text{Bi}, X)$  line at a field of 10 T with  $\vec{H} \parallel [100]$  for

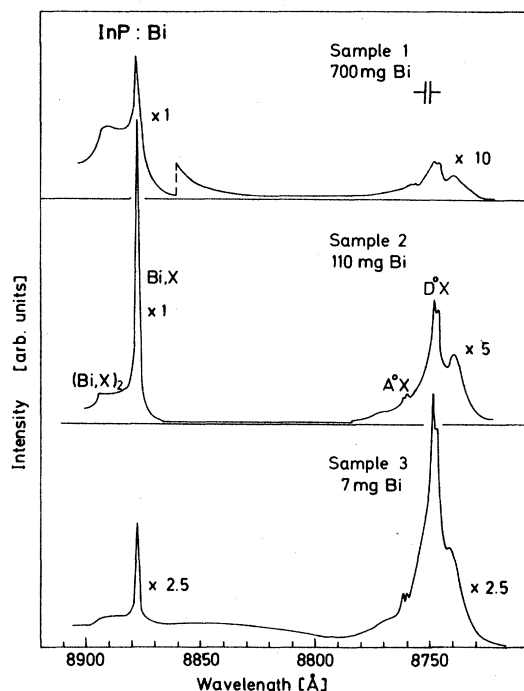


FIG. 1. Photoluminescence spectra at 1.9 K of three InP liquid-phase epitaxial layers with different Bi doping: into the growth melt of about 10-g weight an amount of 7-, 110-, and 700-mg Bi was added for the samples 1, 2, and 3, respectively.  $(D^0, X)$  indicates the decay of donor-bound excitons;  $(A^0, X)$  the decay of acceptor-bound excitons.  $(\text{Bi}, X)$  is the Bi-bound exciton decay. For  $(\text{Bi}, X)_2$ , see text.

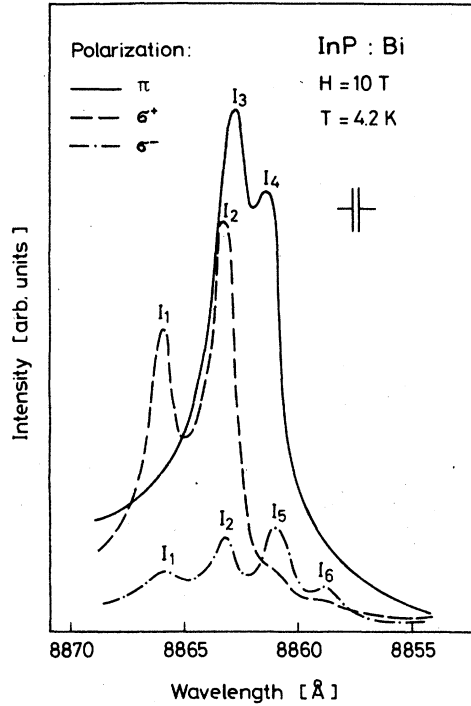


FIG. 2. (Bi,X) emission at a magnetic field of 10 T with  $\pi$  polarization (Voigt configuration) and  $\sigma^+$ ,  $\sigma^-$  polarization (Faraday configuration): a Zeeman splitting into six components ( $I_1$ - $I_6$ ) is observed. The sample was always oriented  $\vec{H} \parallel \langle 100 \rangle$ . The  $\sigma^-$  curve contains still fractions of the  $\sigma^+$  components  $I_1$  and  $I_2$  which are much stronger in intensity and could not be completely suppressed by the filters used.

$\pi$ ,  $\sigma^+$ , and  $\sigma^-$  polarization. A clearly resolved splitting into six strongly polarized components is observed. Figure 3 shows the transition scheme as proposed already by White *et al.*<sup>6</sup>: the electron and hole spin are assumed to be decoupled by the magnetic field (in analogy to the Paschen-Back effect) and each of them undergoes a separate thermalization. The signs of the  $g$  values are now unambiguous because, in contrast to White *et al.*,<sup>6</sup> we were able to perform experiments in Faraday configuration, i.e., we could distinguish between  $\sigma^+$  and  $\sigma^-$  polarization. In good agreement with other experiments<sup>9,12</sup> we obtain an electron  $g_e$  value of

$$g_e = +1.19 \pm 0.05.$$

For the bound hole we obtain for the isotropic and anisotropic  $g$  values in the notation of Ref. 13

$$2\tilde{K} = 0.77 \pm 0.05, \quad 2\tilde{L} = -0.075 \pm 0.01,$$

where  $2\tilde{K} \approx K$  is the isotropic and  $2\tilde{L} \approx L$  the anisotropic part ( $K, L$  are the notation of Ref. 6). These values must be compared with the ones expected

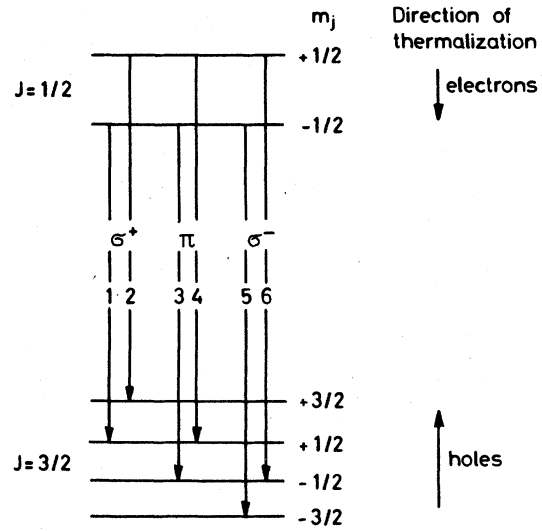


FIG. 3. Transition scheme for decoupled electron ( $J = \frac{1}{2}$ ) and hole ( $J = \frac{3}{2}$ ) spin. To make the selection rules easier to understand ( $\Delta m_j = \pm 1, 0$ ) the split-hole states are drawn as final states, although they undergo a thermalization (see right-hand side of the figure).

theoretically<sup>13</sup> for an effective-mass acceptor. Using the newest experimental valence-band parameters,<sup>14</sup> we obtain for an effective-mass acceptor

$$2\tilde{K} = 2.76, \quad 2\tilde{L} = -0.5.$$

That means that in the case of the Bi-bound hole the  $g$  values are strongly reduced in comparison with the Coulomb-like effective-mass acceptor. This might be expected for a strongly localized hole.<sup>15</sup>

Figure 4 shows the influence of temperature on the relative intensities of the  $\sigma^+$  and  $\sigma^-$  components at 10 T. The lines  $I_5$ ,  $I_1$ , and  $I_6$ ,  $I_2$ , respectively, are transitions with identical electron-spin orientation (compare Fig. 3). Therefore, the ratios  $I_5/I_1$  and  $I_6/I_2$  should obey a Boltzmann law with activation energies equal to the corresponding splitting of the hole states. This is indeed experimentally verified ( $\Delta E_{\text{thermal}} = 0.77$  meV;  $\Delta E_{\text{optical}} = 0.74$  meV). That means the holes thermalize with the sample temperature before recombination takes place.

The easiest way to examine the thermalization of the electrons would be a comparison of transitions involving the different electron states but the same hole state (e.g.,  $I_1$  and  $I_4$  in Fig. 3). However, this means a comparison of  $\sigma$  and  $\pi$  components, which is experimentally difficult. An evaluation is also possible if the intensities  $I_2/I_1$  in the well resolved  $\sigma^+$  spectrum are considered and if the known thermalization of the holes is

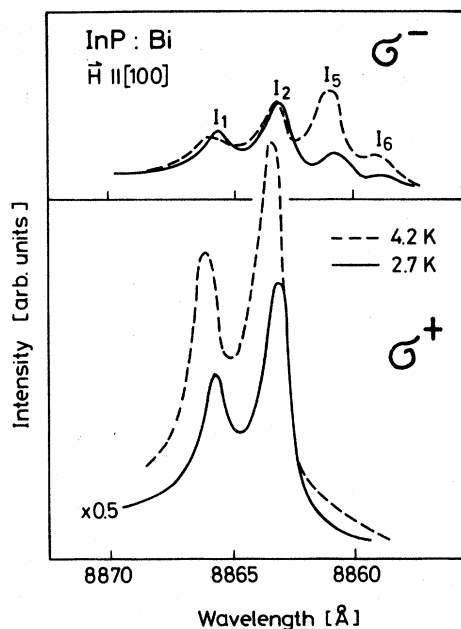


FIG. 4. Temperature dependence of the  $\sigma^+$  and  $\sigma^-$  spectra: spectra at 4.2 (dashed) and 2.7 K (straight line) are shown at a magnetic field of 10 T with  $\vec{H} \parallel (100)$ . As in Fig. 2, the  $\sigma^-$  curve contains portions of the  $\sigma^+$  components.

taken into account. Assuming a Boltzmann distribution, the following expression holds for the temperature dependence of the intensity ratio

$$I_2/I_1 \sim \exp(-\Delta E_e/kT) \times \exp(+\Delta E_h/kT), \quad (1)$$

where  $\Delta E_e$  and  $\Delta E_h$  are the absolute values of the known electron and hole splittings and  $T$  is the temperature.  $\Delta E_e$  is by a factor of 2.4 larger than  $\Delta E_h$ , and hence the ratio  $I_2/I_1$  should increase by a factor of 2 if the bath temperature is increased from 2.7 to 4.2 K. It can be clearly seen from Fig. 4 (lower part) that the reverse case is observed experimentally:  $I_2/I_1$  decreases with increasing temperature due to the second Boltzmann-factor in Eq. (1), i.e., due to the thermalization of the holes only. This means that no electron-spin thermalization takes place, i.e., the spin-lattice relaxation time at this magnetic field (10 T) for a bound electron must be larger than the radiative decay time (several hundred nsec, see below).

Similar observations, that the electron spin does not thermalize in quantizing magnetic fields, have been made for excitons strongly bound to neutral acceptors in GaSb.<sup>16,17</sup> It was proposed that the spin relaxation in the conduction band of a noncentrosymmetric III-V compound is dominated by the spin-orbit splitting of electron states corresponding to  $k \neq 0$ , whereas the bound-electron

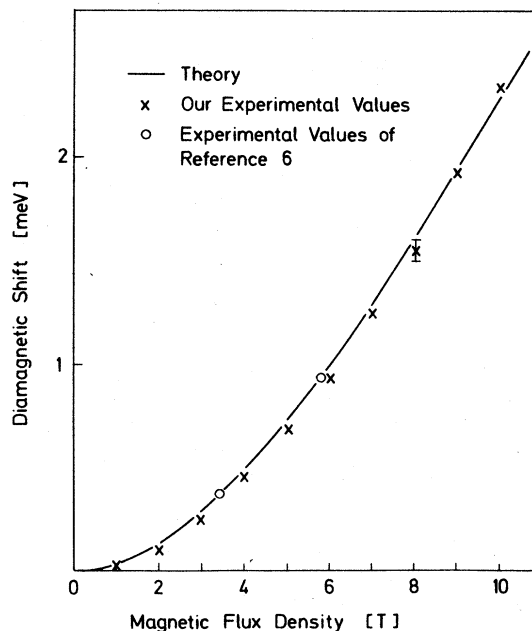


FIG. 5. Comparison of the diamagnetic shift of the sharp (Bi, X) line (crosses) with the diamagnetic shift of a donor in InP (after Ref. 18). The experimental values of Ref. 6 (circles) are given too.

state undergoes nearly no thermalization.<sup>17</sup> We conclude that although the general thermalization may be very fast, spin thermalization must have long time constants ( $>200$  nsec).

We now discuss the diamagnetic effects of the (Bi, X) line. Figure 5 shows the experimental values (crosses) for the diamagnetic shift, i.e., the shift of the center of gravity of all the observed Zeeman split components. These experimental values are compared with the theoretical shift of a donor in InP after Cabib *et al.*<sup>18</sup> with  $m^*/m_0 = 0.081$ ,<sup>19</sup> and a dielectric constant of  $\epsilon_0 = 12.1$ .<sup>5</sup> Surprisingly, this theoretical curve fits the experimental data extremely well, demonstrating that the (Bi, X) state behaves like a donor (pseudo-donor), i.e., the hole does not contribute to the observed diamagnetic shift.

A further experimental result confirms the strong localization of the hole: the asymmetry of the Zeeman splitting is very small (compare, e.g., the  $\sigma^-$  components in Fig. 2). The asymmetry is caused by a different diamagnetic shift of the  $|m_j| = \frac{3}{2}$  and  $|m_j| = \frac{1}{2}$  hole states. This "diamagnetic splitting" should be proportional to the square of the radius of the hole-wave function.<sup>13</sup> The small experimentally observed diamagnetic splitting (only  $0.036 \pm 0.015$  meV at 10 T) therefore proves that the hole is extremely localized.

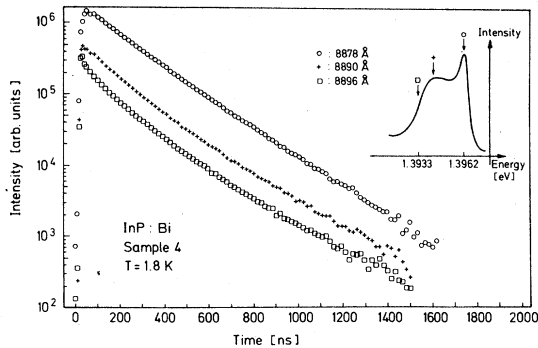


FIG. 6. Time dependence of the luminescence intensity at three different wavelengths: (a) at the  $(\text{Bi}, X)$  line, 8878 Å ( $\circ$ ); (b) at the low-energy shoulder, 8890 Å ( $+$ ) and 8896 Å ( $\square$ ). The positions of the different wavelengths are given in the insert.

## 2. Time-resolved measurements

Figure 6 shows the time dependence of the Bi luminescence at three different wavelengths. The insert in the figure shows that the circles are values taken at a wavelength corresponding to the peak position of the Bi exciton, whereas the other symbols correspond to two positions at the low-energy  $(\text{Bi}, X)_2$  emission. All three lifetimes are essentially equal and are of the order of magnitude of 200 nsec. The decay at all three different wavelengths is not completely exponential. At short times after the excitation pulse, the long-wavelength decay (lowest curve) is more rapid. The long-time decay is practically identical for all the different wavelengths. The initial different decay times cause a variation of the line shape of spectra taken at different delay times after the excitation pulse. These time-resolved spectra are depicted in Fig. 7: the decay of the  $(\text{Bi}, X)_2$  emission is slightly more rapid than that of the Bi exciton. In addition, a shift in peak energy and line shape of the  $(\text{Bi}, X)_2$  emission may be observed. This is discussed later in connection with the intensity dependence of that emission.

The lifetime of about 200 nsec is much larger than those observed for excitons bound to neutral donors or acceptors in direct-gap semiconductors (InP: 0.5 and 1.5 nsec, respectively<sup>7</sup>). A similar behavior has been observed for the case of CdS:Te.<sup>20</sup> Henry and Nassau<sup>20</sup> tried the following theoretical approach to calculate the lifetime of bound excitons and donor-acceptor pair recombination: they related the different oscillator strengths of free and bound excitons as well as of pair spectra by comparison of the overlap of the hole and electron wave functions in the three cases. One simplifying assumption in their calculations is that the extension of the hole wave function is

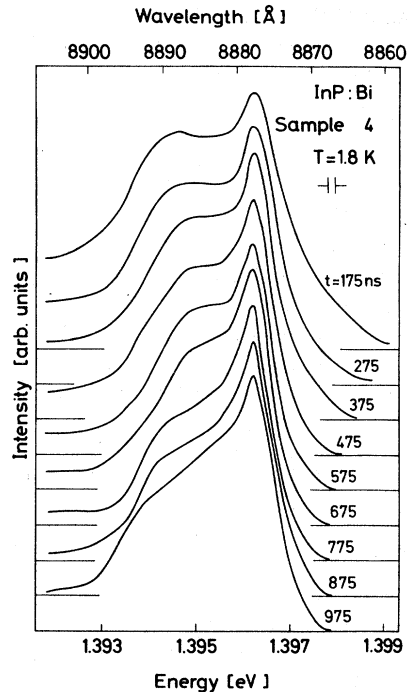


FIG. 7. Spectra taken at different delay times after a short-excitation pulse. The delay times are, respectively, indicated in the picture.

much smaller than that of the electron. Since, for InP, this assumption is also justified, the theory in principal could be adopted for the case of InP:Bi.

A further assumption of Henry and Nassau is that effective-mass theory can be applied even in the case of the strongly localized hole of the isoelectronic impurity: in calculating the extension of the Te-bound hole they use a hole mass calculated from an acceptor-binding energy in CdS in the framework of effective-mass theory. However, this is not correct. As a consequence they did not get agreement between theoretically estimated and experimentally observed decay times for the Te-bound exciton in CdS.

For this reason we proceed in the opposite way: from the measured lifetime we calculate the spatial extension and thereby the mass of the Bi-bound hole in InP. Starting from the measured lifetime of donor-acceptor pair recombination involving the effective-mass-like acceptor Zn, using the newest obtainable valence-band parameters<sup>14</sup> and the effective-mass theory for acceptors in the case of degenerated valence bands<sup>21, 22</sup> we obtain for the oscillator strength of the free exciton (per InP molecule volume) (see the Appendix)

$$f_{\text{ex}} = 3.32 \times 10^{-5} \text{ cm}^2/\text{sec}.$$

Assuming that the hole is bound by a short-range square-well potential, its ground-state envelope function outside this potential is described by

$$\Phi_h = (+2\pi\lambda)^{-1/2} e^{-r/\lambda}/r, \quad (2)$$

where

$$\lambda = (\hbar^2/2m_h E)^{1/2} \quad (3)$$

is a measure for the extension of the hole. This expression can be obtained in a straightforward way by using a spherically symmetric square-well potential ( $V = V_0$  for  $r > a$ ,  $V = 0$  for  $r < a$ ). Comparing the time constants of the pair recombination and the Bi-bound hole we get an equation<sup>20</sup> for  $\lambda$ :

$$\lambda = 2a_A \left( \frac{\tau_{DA}^{\min} \hbar\omega(\text{Bi}, X)}{\tau_{(\text{Bi}, X)} \hbar\omega_{DA}} \right)^{1/3}. \quad (4)$$

With the experimental values we obtain

$$\lambda = 12.8 \text{ \AA}.$$

This value means a surprisingly strong localization of the hole: for comparison the radius of the hole at the effective-mass acceptor has the value 33 \AA, whereas its localization energy is 46 meV.<sup>14, 22</sup> The experimentally determined localization energy of the hole at Bi is  $E = 19.6$  meV. From Eq. (3) we can calculate the effective mass of the Bi-bound hole to be

$$m_h = 1.19m_0,$$

a mass which is much larger than the band-edge effective masses. This result is well understood considering the whole problem from another point of view: strong localization of the hole in real space means a large spread in  $k$  space. Therefore, not the band-edge effective mass determines the translational energy of the hole, but a mass averaged over a large extension of the valence band in  $k$  space. This mass, however, is, in any case, larger than the band-edge mass due to the nonparabolicity of the valence band.

Another experimental result that has already shown is that the hole is strongly localized and/or has a larger effective mass than the band-edge mass; no diamagnetic shift of the hole was observed in the magnetic-field experiments.

To summarize: the lifetime measurements also confirm our pseudodonor model, i.e., the strong localization of the hole.

Let us postpone the discussion of the time dependence of the  $(\text{Bi}, X)_2$  emission and continue now discussing the features of the  $(\text{Bi}, X)$  exciton.

### 3. Temperature dependence

Figure 8 shows the temperature dependence of the integrated intensity  $I_{NP}$  of the zero-phonon line

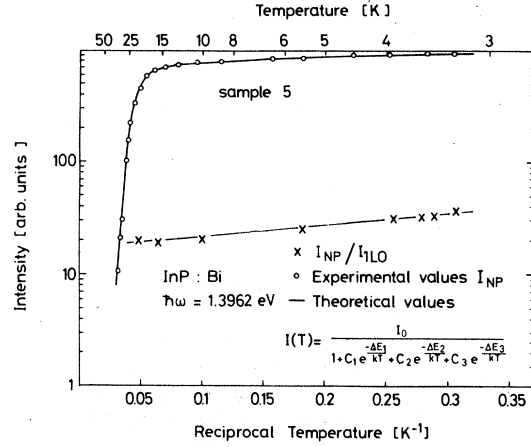


FIG. 8. Fit of the temperature dependence of the intensity of the zero-phonon line  $I_{NP}$  of the Bi "exciton" (circles) according to the formula given in the picture. The crosses, connected by the dashed straight line are experimental values for  $I_{NP}/I_{1LO}$ , i.e., they give an impression of the temperature dependence of the phonon coupling.

of the Bi exciton. Two different temperature regions can be distinguished at once: at low temperatures up to 10 K a slight decrease, above 25 K a very rapid decrease is observed.

Let us first discuss the low-temperature regime: Due to the strong localization of the hole, the surrounding lattice is strongly polarized. If recombination takes place, i.e., the Bi atom becomes neutral, the lattice relaxes back to its undeformed unpolarized state, i.e., phonon emission takes place. Now the phonon coupling of the transition (given by the intensity ratio of the 1LO-phonon replica and the zero-phonon line) is not only large ( $I_{1LO}/I_{NP} = 0.5$  for  $T = 10$  K), but also temperature dependent. This temperature dependence is shown by the crosses in Fig. 8, which are experimental values of the intensity ratio  $I_{NP}/I_{1LO}$ . Although a quantitative description of this temperature-dependent phonon coupling is very difficult, at least qualitatively the increase of the phonon coupling with increasing temperature is expected.

With increasing temperature the lattice atoms begin to oscillate around their equilibrium positions (excitation of acoustical phonons). The mean position of the atoms, however, remains constant if the corresponding potential is symmetric as in the case of a cubic lattice. However, if the Coulomb field of the  $\text{Bi}^+$  state is superimposed, the potential becomes asymmetric: the positively charged atoms are repulsed and the negative ones are attracted with a  $1/r$  law. As a consequence, the mean position of the positive and negative charges changes with increasing temperature:

the induced dipole moments are augmented in comparison to the  $T=0$  case, i.e., the polarization of the lattice becomes larger with temperature and therefore the phonon coupling in the transition increases too.

In conclusion, the slow decrease of the intensity of the zero-phonon line in the range up to 10 K is due to an increase of the phonon coupling: the *total* intensity of the zero-phonon line and all the phonon replica remains nearly constant in this temperature regime, i.e., no ionization of the Bi exciton takes place.

Next we discuss the high-temperature regime. Above 25 K a rapid decrease in intensity is observed yielding an activation energy of 28 meV. This energy corresponds to the complete ionization of the Bi exciton generating a free electron and hole, and it agrees with optically determined values.

Between these two extreme temperature regions the activation of the electron only ( $\Delta E_2 = 7.4$  meV) is observed.

These three possible processes for the intensity decrease of the zero-phonon line can be expressed mathematically by the formula given in Fig. 8.<sup>23</sup>  $\Delta E$  gives the activation energy and the prefactor  $C$  describes how efficiently the activation reduces the luminescence intensity. For the best fit we obtain

$$\Delta E_1 = 0.75 \text{ meV}, \quad C_1 = 0.655,$$

$$\Delta E_2 = 7.4 \text{ meV}, \quad C_2 = 26.6,$$

$$\Delta E_3 = 28 \text{ meV}, \quad C_3 = 2.7 \times 10^6.$$

Large  $C$  means that the dissociation process is very efficient. It turns out that the ionization of the electron alone (small  $C_2$ ) is not very efficient, due to the fact that the  $\text{Bi}^*$  center quickly can recapture another electron. However, the liberation of both (electron and hole) decreases the Bi luminescence efficiently with respect to other competing recombination processes.  $C_1$  and  $\Delta E_1$  describe the increase in phonon coupling.

#### 4. Absorption experiments

Figure 9 shows the transmission spectrum of the Bi-doped epitaxial layer. The insert shows the interesting wavelength region but with a zero suppression of a factor of 10 (please note the different wavelength scales!).

The experimentally determined integral absorption  $\int \alpha dE$  together with the experimentally determined oscillator strength from decay measurements allows us to calculate a Bi concentration ( $N_{\text{Bi}} = 5 \times 10^{15} \text{ cm}^{-3}$  for this sample, see Sec. II A).

The most interesting result of the absorption

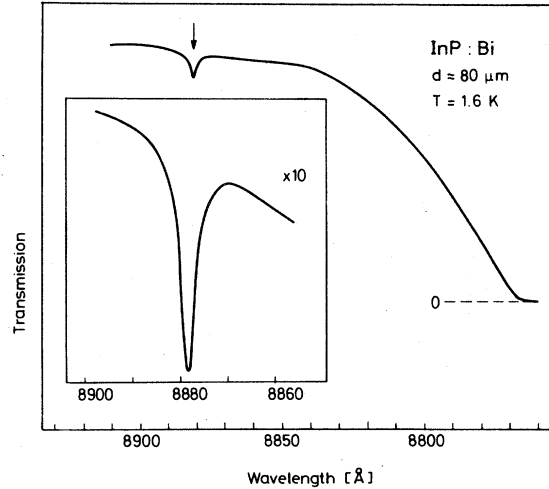


FIG. 9. Transmission spectrum of a Bi-doped LPE layer. In the insert the Bi absorption is given with a zero suppression of a factor of 10. Please, note the different wavelength scales!

measurement is that the  $(\text{Bi}, X)_2$  line, always observed in emission, does not appear in the transmission spectrum. This experimental observation leads us directly to Sec. III. B in which the origin of this  $(\text{Bi}, X)_2$  emission is discussed.

#### B. Discussion of the low-energy emission $(\text{Bi}, X)_2$

We considered three possibilities to explain the appearance of the low-energy satellite  $(\text{Bi}, X)_2$  of the sharp Bi exciton.

(a) The  $(\text{Bi}, X)_2$  line is a phonon wing of the sharp Bi line: the strongly localized hole has a large extension in  $k$  space and therefore an acoustical-phonon contribution might conserve the momentum in the transition. A corresponding acoustical-phonon wing was found, e.g., for the  $I_1$  line  $(A^0, X)$  in CdS.<sup>24</sup>

(b) The  $(\text{Bi}, X)_2$  line is a pair spectrum of a neutral donor and a Bi-bound hole ( $D^0, \text{Bi}^*$ ). Such a transition is assumed to take place in GaP doped with both Bi and different donors (Te, S, Se).<sup>3</sup>

(c) The  $(\text{Bi}, X)_2$  line is due to Bi-exciton pairs, i.e., *two* excitons are bound at a Bi-Bi pair. Due to the large differences in electron and hole localization these *exciton* pairs can be very simply treated in a direct analogy to the  $\text{H}_2$  molecules. These pairs must be distinguished from the NN isoelectronic pairs found in very highly doped GaP:N.<sup>25</sup> In the GaP:N case only *one* exciton is bound by a NN pair.

We shall now exclude the first two possibilities and demonstrate that the third interpretation correctly describes all the experimentally observed behavior of the  $(\text{Bi}, X)_2$  line. Figure 10 clearly

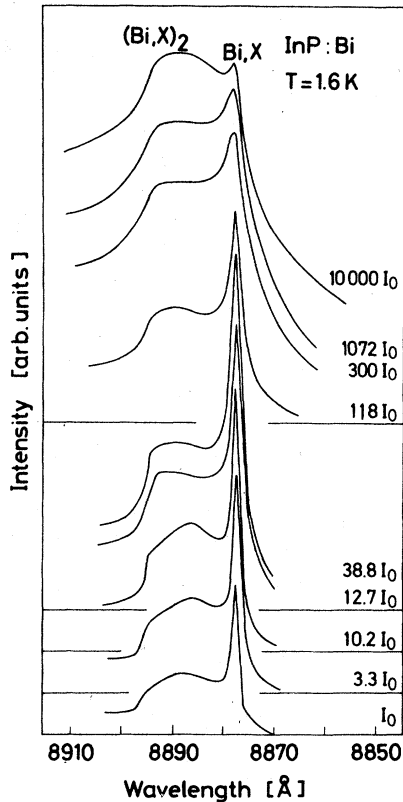


FIG. 10. Dependence of the line shape of the Bi emission on the intensity of dc excitation.  $I_0$  was about  $10^{-5}$  W/cm $^2$ .

demonstrates that the first interpretation (acoustical-phonon wing) can be excluded: the intensity ratio of the two emission bands strongly changes if the excitation intensity is increased. This is, at least in a first approximation, not expected for a phonon wing. In addition, Fig. 1 shows that for different Bi doping the relative intensities change too, which is also not consistent with the phonon-wing interpretation of the  $(\text{Bi}, X)_2$  line.

The second interpretation (donor- $\text{Bi}^+$  pair transition) can be excluded by similar arguments.

(a) The intensity of the  $(\text{Bi}, X)_2$  line is only connected with the Bi and not with the donor concentration. In Fig. 1 the  $(\text{Bi}, X)_2$  intensity increases from bottom to top where only the Bi concentration changes and the donor concentration is approximately constant (equal linewidth and intensity ratios of the  $(D^0, X)$  and  $(A^0, X)$  emission in all three cases).

(b) For  $n$ -type samples, the number of donor-Bi pairs and isolated Bi-pseudodonor is only given by the doping concentrations and should not vary with excitation intensity if the two transitions have nearly identical decay times (as shown in Sec. IIIA). However, as demonstrated by Fig. 10, the re-

verse behavior is observed: for high Bi doping the  $(\text{Bi}, X)_2$  line increases strongly its relative intensity with increasing excitation power.

(c) As mentioned, the decay behavior of both lines is essentially identical: for  $(\text{Bi}, X)_2$  no time dependence corresponding to a pair recombination as in the case of GaP:Bi (Ref. 3) is observed (see Fig. 6).

One might argue that this difference originates from the following fact: due to the light electron mass in InP the  $(D^0, \text{Bi}^+)$  pair resembles an  $\text{H}_2^+$  molecule, i.e., the electron is equally distributed at both positive centers. This is in principal correct, however, even in this model the decay time of the  $(D^0, \text{Bi}^+)$  line should be twice that of the  $(\text{Bi}, X)$  line since then the electron is distributed equally between the  $\text{Bi}^+$  and  $D^+$ -center.

(d) The maximal decrease of energy in the  $\text{H}_2^+$  molecule is 0.206 Ry, i.e., 1.5 meV in InP. The experimentally observed decrease, however, is larger, namely, 2.5 meV.

This last argument *against* the interpretation of the  $(\text{Bi}, X)_2$  line as the decay of  $(D^0, \text{Bi}^+)$  pairs leads us directly to an argument for the third interpretation, that the  $(\text{Bi}, X)_2$  line is due to the decay of Bi-exciton pairs, or, otherwise expressed, pseudodonor molecules resembling an  $\text{H}_2$  molecule with fixed distance of the positive nuclei: (a) the experimentally observed energy position of the  $(\text{Bi}, X)_2$  is 2.45 meV below the  $(\text{Bi}, X)$ . This value corresponds to 0.321 Ry, i.e., approximately the binding energy of the  $\text{H}_2$  molecule in InP. The other arguments for this last interpretation are (b) The  $(\text{Bi}, X)_2$  emission depends on Bi doping only. (c) In absorption no  $(\text{Bi}, X)_2$  line is observed, since no  $(\text{Bi}, X)$ -Bi pairs are present in the unexcited state. (d) The lifetime behavior of the  $(\text{Bi}, X)_2$  emission is understood in the pseudodonor molecule picture. (e) The changes in the line shape with increasing excitation density are explained by this model.

The last two points need a further more detailed explanation.

### 1. Time constants

The probability that one of the two  $(\text{Bi}, X)$  states of a  $(\text{Bi}, X)_2$  molecule decays is twice that of a single  $(\text{Bi}, X)$  state. With the decay of a  $(\text{Bi}, X)_2$  state one single, isolated  $(\text{Bi}, X)$  state is created. Therefore, the expected decay behavior is the following: the  $(\text{Bi}, X)_2$  emission must decay more rapidly accompanied by an increase of  $(\text{Bi}, X)$



emission. Figure 6 demonstrates that this is indeed experimentally observed at short times (<150 nsec) after the excitation pulse.

The long-time decay is equal for both emissions and therefore may be described by one time constant. We suggest that this long-time decay is governed by the decay time of the isolated  $(\text{Bi}, X)$  exciton. The pair states at lower energies are filled up by tunneling of excitons from Bi to Bi atom. Indeed, at the present Bi concentrations the tunneling process time is at least comparable to the decay time.

For the tunneling time  $\tau_t$  the following equation is valid

$$\tau_t = (2\pi^2/\omega_0)e^{+2R/\lambda},$$

where  $\lambda$  is the hole extension (see Sec. IIIA),  $R$  the distance between the Bi atoms, and  $\omega_0$  the depth of the hole-binding potential. Taking reasonable values ( $\lambda = 13 \text{ \AA}$ ,  $R_0 = 100 \text{ \AA}$  for  $N_{\text{Bi}} \lesssim 10^{18} \text{ cm}^{-3}$ ,  $\hbar\omega_0 = 1 \text{ eV}^1$ ) we obtain  $\tau_t = 60 \text{ nsec}$ .

## 2. Line shape in dependence on excitation

The behavior of the  $(\text{Bi}, X)_2$  line with increasing dc excitation is qualitatively well understood in the  $\text{H}_2$  molecule model: intensity increase of the  $(\text{Bi}, X)_2$  line is more rapid than the  $(\text{Bi}, X)$  emission (Fig. 10), since, at the higher-excitation level isolated Bi excitons become more and more seldom compared to  $(\text{Bi}, X)_2$  pairs.

For an accurate line-shape analysis of the  $(\text{Bi}, X)_2$  line we prefer to use spectra taken at pulsed excitation (pulse to repetition time ratio of  $1:10^4$ ) for the following reason: in this case the long-living Bi lines show a sharper structure, due to a strong reduction of broadening processes like interactions with photocreated free carriers and other short-living excitations.

On the right-hand side of Fig. 11 the line shapes of the  $(\text{Bi}, X)_2$  emission are given at different pulsed-laser powers (the average powers are given in the pictures, respectively). The contribution of the sharp Bi exciton emission was subtracted, assuming that this sharp line is symmetric, which allows an unfolding of the two emission bands. The theoretical line shapes on the left-hand side were calculated according a very simple model.

The energy decrease of a recombination in a pair relative to the isolated Bi pseudodonor is assumed to follow a simple Morse potential (in direct analogy to the  $\text{H}_2$  molecule).

$$U(r) = -D + D\{1 - \exp[-a(r - r_0)]\}^2. \quad (5)$$

Using atomic units in Eq. (5) reduced to the case of InP we obtain a relation  $E(r)$  between energy

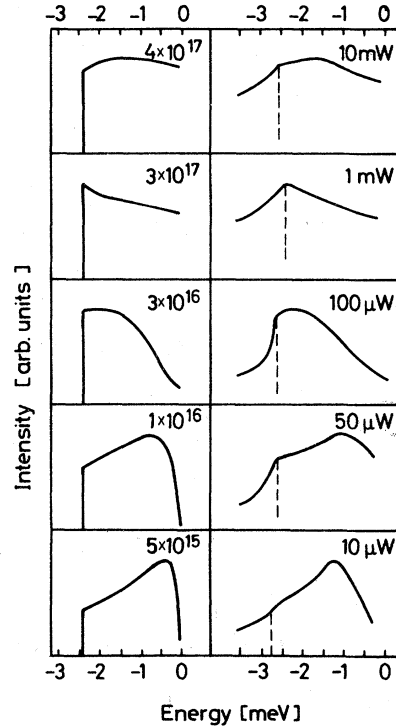


FIG. 11. Comparison of the experimental line shape at different pulsed excitation (the average power is given, respectively, on the right-hand side) with the theoretical line shape of "pseudodonor molecules" at different pseudodonor concentrations (left-hand side).

$E$  of the emitted photon and pair distance  $r$ . Now the probability to find at a concentration  $N$  of Bi excitons (i.e., *excited* Bi atoms) a pair with a distance  $r$  and no closer pair is given by<sup>26</sup>

$$W(r) = 4\pi r^2 N \exp(-\frac{4}{3}\pi r^3 N). \quad (6)$$

Assuming equal decay probabilities for all pair separations (a very crude assumption as shown before), line shapes can be calculated with the concentration  $N$  of Bi excitons as parameter.

In Fig. 11, on the left-hand side, the line shapes are shown for various  $N$ . The agreement between theoretical and experimental line shapes is rather good considering the simplicity of the model: although the abrupt decrease of the low-energy side of the theoretical line is smeared out in the experimental spectra (due to interactions), for the four lowest spectra  $N$  must be increased by nearly the same amount as the laser power is increased (both are increased by two orders of magnitude). At the highest excitation (the uppermost spectra) obviously a saturation takes place: since only about  $4 \times 10^{17}$  Bi atoms per  $\text{cm}^3$  are present, no increase of Bi excitons above this number is possible.

Let us at this point emphasize once more the difference between the NN-pair lines in GaP:N and the pseudodonor molecule picture, used here: In the case of GaP:N *one* exciton is bound in the two potentials of two N atoms, whereas in our case *two* excitons are bound by the two Bi atoms. There are two essential differences between the two systems.

(i) The hole wave function in the case of InP:Bi is more strongly localized for InP:Bi than the electron wave function in GaP:N, i.e., an energy decrease of the bound hole would be only obtained for extremely close pairs in InP:Bi. This, however, would require Bi concentrations which are several orders of magnitude larger than it is the case for our samples.

(ii) On the other hand, the electron wave function in the case of Bi-bound excitons in InP is much more spread than the hole wave function for GaP:N, i.e., electron interaction for (Bi, X)-(Bi, X) pairs is much more important in InP than hole-hole interaction of (N, X)-(N, X) pairs in GaP.

The present Bi concentrations in InP are still too low to observe lines in the luminescence spectrum which are due to the decay of *one* exciton bound to two Bi atoms.

In addition, several experimental observations reported in this paper makes an interpretation of the (Bi, X)<sub>2</sub> line as the decay of one exciton bound to two, very close Bi atoms impossible: e.g., the dependence on excitation intensity of the (Bi, X)<sub>2</sub> line (see Fig. 10) should be just the opposite, due to saturation of the close Bi pairs.

To summarize this section: all the time-, excitation-, and doping-dependent properties of the (Bi, X)<sub>2</sub> line are consistently and satisfactorily described only by the pseudodonor molecule model in which two (Bi, X) excitons form an H<sub>2</sub>-like molecule state. Similar states have been found in the case of neutral donor-pair molecules.<sup>28,29</sup>

#### ACKNOWLEDGMENTS

The financial support of the Deutsche Forschungsgemeinschaft in the framework of the

SFB 67 is gratefully acknowledged. The magnetoluminescence was performed at the Hochfeldmagnetlabor des Max-Planck-Instituts für Festkörperforschung in Grenoble. The authors are grateful for discussions and contributions of their colleagues D. Bimberg and K. Hess.

#### APPENDIX: CALCULATION OF THE OSCILLATOR STRENGTH OF THE FREE EXCITON FROM THE DECAY BEHAVIOR OF DONOR-ACCEPTOR PAIRS

We followed the analysis of Henry and Nassau.<sup>20</sup> From the experimentally determined, extrapolated lifetime  $\tau_{\min}$  for close pairs ( $R \rightarrow 0$ ), one obtains for the oscillator strength<sup>20</sup>

$$f_{DA} e^{2R/a_D} (R=0) = 4.50 \lambda_{DA}^2 / n \tau_{\min},$$

where  $\lambda_{DA}$  is the wavelength of the transition in cm,  $n$  the refractive index, and  $a_D$  the donor Bohr radius.

We use the lifetime  $\tau_{\min} = 1.4 \times 10^{-8}$  sec of the donor-acceptor recombination involving the acceptor Zn which is closest to the effective-mass acceptor: its 1s and 2s acceptor binding energies (46.1 and 13.9 meV) correspond nearly exactly<sup>27</sup> to those of the effective-mass acceptor calculated with the theory of Baldereschi and Lipari.<sup>21,22</sup> From the same theory we obtain the mean extension of the acceptor wave function to be

$$\langle r_A \rangle = 33 \text{ \AA}.$$

It is assumed that the calculation is still valid in the case of degenerate valence bands with acceptor wave functions which are not hydrogen-like, if the acceptor Bohr radius  $a_A$  is replaced by  $\langle r_A \rangle$ .

The situation becomes even more complicated if one deals with an acceptor which is not effective masslike; e.g., a more shallow acceptor ( $E_A = 41$  meV) in InP (probably carbon) shows a much shorter  $\tau_{\min}$ ,<sup>27</sup> indicating a much larger extension of the acceptor wave function.

\*Present address: Robert Bosch GmbH, Stuttgart.

†Present address: Wacker Chemitronic, Burghausen.

‡Present address: Battelle Institute, Frankfurt.

<sup>1</sup>A. Baldereschi, *J. Lumin.* **7**, 79 (1973), and references therein.

<sup>2</sup>P. J. Wiesner, R. A. Street, and H. D. Wolf, *J. Lumin.* **12-13**, 265 (1976), and references therein.

<sup>3</sup>P. J. Dean, J. D. Cuthbert, and R. T. Lynch, *Phys. Rev.* **179**, 754 (1969).

<sup>4</sup>D. G. Thomas, *IEEE Trans. Electron Devices* **18**, 621 (1971).

<sup>5</sup>P. J. Dean, A. M. White, E. W. Williams, and M. G. Astles, *Solid State Commun.* **9**, 1555 (1971).

<sup>6</sup>A. M. White, P. J. Dean, K. M. Fairhurst, W. Bardsley, and B. Day, *J. Phys. C* **7**, L35 (1974).

<sup>7</sup>U. Heim, *Phys. Status Solidi*, **B 48**, 629 (1971).

<sup>8</sup>R. C. Clarke and L. L. Taylor, *J. Cryst. Growth* **31**, 190 (1975).

<sup>9</sup>K. Hess, N. Stath, and K. W. Benz, *J. Electrochem. Soc.* **121**, 1208 (1974).

<sup>10</sup>R. Hultgren, P. D. Dersay, D. T. Hawkins, M. Gleiser, and K. K. Kelley, in *Properties of Binary Alloys*

- (American Society for Metals, Cleveland, 1973), p. 418.
- <sup>11</sup>W. Klingenstein (unpublished).
- <sup>12</sup>C. Weisbuch, C. Hermann, and G. Fishman, in *Proceedings of the International Conference on the Physics of Semiconductors, Stuttgart, 1974* (Teubner, Stuttgart, 1974), p. 761.
- <sup>13</sup>W. Schairer, D. Bimberg, W. Kottler, K. Cho, and Martin Schmidt, *Phys. Rev. B* **13**, 3452 (1976).
- <sup>14</sup>D. Bimberg, K. Hess, N. O. Lipari, J. U. Fischbach, and M. Altarelli, *International Conference on Magneto-Optics, Zürich, 1976*, edited by P. Wachter (North-Holland, Amsterdam, 1977), p. 139.
- <sup>15</sup>T. Morgan, *J. Lumin.* **1-2**, 420 (1970).
- <sup>16</sup>W. Rühle and D. Bimberg, *Phys. Rev. B* **12**, 2382 (1975).
- <sup>17</sup>B. P. Zakharchenya, E. L. Ivchenko, A. Ya. Ryskin, and A. V. Varfolomeev, *Sov. Phys. Solid State* **18**, 132 (1976).
- <sup>18</sup>D. Cabib, E. Fabri, and G. Fiorio, *Nuovo Cimento B* **10**, 185 (1972).
- <sup>19</sup>J. M. Chamberlain, H. B. Ergun, K. A. Gehring, and R. A. Stradling, *Solid State Commun.* **9**, 1563 (1971).
- <sup>20</sup>C. H. Henry and K. Nassau, *Phys. Rev. B* **1**, 1628 (1970).
- <sup>21</sup>A. Baldereschi and N. O. Lipari, *Phys. Rev. B* **8**, 2697 (1973).
- <sup>22</sup>A. Baldereschi and N. O. Lipari, *Phys. Rev. B* **9**, 1525 (1974).
- <sup>23</sup>D. Bimberg, M. Sondergeld, and E. Grobe, *Phys. Rev. B* **4**, 3451 (1971).
- <sup>24</sup>J. J. Hopfield, *Proceedings of the International Conference on the Physics of Semiconductors, Exeter, 1962*, (Institute of Physics and Physical Society, London, 1962), p. 75.
- <sup>25</sup>P. J. Wiesner, R. A. Street, and H. D. Wolf, *J. Lumin.* **12-13**, 265 (1976).
- <sup>26</sup>F. Williams, *Phys. Status Solidi* **25**, 493 (1968).
- <sup>27</sup>R. Meck, M. Pilkuhn (unpublished).
- <sup>28</sup>J. Golka, *J. Phys. C* **7**, L407 (1974).
- <sup>29</sup>L. V. Berman, *Sov. Phys. Semicond.* **10**, 358 (1976).